Synthesis and Properties of a Novel Series of Organometallic Merocyanines Combining the Potent Electron-Donating $[(CpFeCO)_2(\mu\text{-}CO)(\mu\text{-}C{=}CH{-})]$ Fragment with Tropylium-Type Acceptors

Tony Farrell,*[a] Anthony R. Manning,*[a] Gemma Mitchell,[a] Jürgen Heck,*[b] Timo Meyer-Friedrichsen,[b] Maik Malessa,[b] Christian Wittenburg,[b] Marc H. Prosenc,[b] Des Cunningham,[c] and Pat McArdle[c]

Dedicated to Prof. Dr. Gottfried Huttner on the occasion of his 65th birthday

Keywords: Organometallic compounds / Merocyanines / Azulenes / Bond length alternation / Solvatochromism / Nonlinear optics (NLO) / Long-wavelength hyper-Rayleigh scattering (HRS)

The potent electron-donating group $[(CpFeCO)_2(\mu\text{-}CO)(\mu\text{-}C{=}CH{-})]$ was combined with different tropylium-based acceptors yielding the push-pull complexes $[(CpFeCO)_2(\mu\text{-}CO)(\mu\text{-}C{=}CH{-}CH{=}A)][BF_4]$ where =A represents $[{=}CH{-}(\eta^7\text{-}C_7H_6)Cr(CO)_3]^+$ (**5**), $[{=}\{C_{10}H_7\}]^+$ (azulenylium) (**7**) $[{=}\{C_{10}H_4Me_2iPr\}]^+$ (guaiazulenylium) (**8**). Crystal structures of the precursor complexes $[(CpFeCO)_2(\mu\text{-}CO)(\mu\text{-}C{=}CH{-}CH{=}CH{-}C_7H_7)]$ (**3**), $[(CpFeCO)_2(\mu\text{-}CO)\{\mu\text{-}C{=}CH{-}CH{=}CH{-}(\eta^6\text{-}C_7H_7)Cr(CO)_3\}]$ (**4**) and the push-pull derivative **5** are presented. Whereas complexes **3** and **4** demonstrate localised carbon–carbon double and single bonds in the π-bridge between the diiron moiety and the seven-membered ring a small but distinct π-bond delocalisation can be observed in the π-linker of the cationic derivative **5**. From the NMR spectroscopic results a correlation between the ^{13}C NMR shift of the bridging carbon atom μ-C of the diiron unit and the coupling constant $J(^1H\text{-}^1H)$ of the β- and γ-protons of the π-bridge was found. This correlation indicates an increased π-bond delocalisation throughout the conjugated bridge with respect to the electron-accepting capability in the order tricarbonyl(η^7-cycloheptatrienylium)chromium < guaiazulenylium < azulenylium implying a predominantly charge-delocalised form in the case of the azulenylium complex **7**. Considerably large first hyperpolarisabilities β were determined for **5** and **8** by means of hyper-Rayleigh scattering. Based on the two-level model β_0 values were calculated and related to the bond-length alternation in the π-linker.

Introduction

A major feature of the research into materials capable of doubling the frequency of incident light (second harmonic generation, SHG), a second-order nonlinear optical (NLO) property, is the determination of the first hyperpolarisability β.[1] Dipolar chromophores of the form D−π−A are the most important class of compounds capable of frequency doubling, where D represents an electron donor, A an electron acceptor and a π-bridge of unsaturated bonds providing the electronic communication between the termini. One of our approaches has been to synthesise organometallic merocyanine complexes which utilise the cationic diiron $[(CpFeCO)_2(\mu\text{-}CO)(\mu\text{-}C{-})]^+$moiety as an electron acceptor[2] and the related μ-vinylidene $[(CpFeCO)_2(\mu\text{-}CO)(\mu\text{-}C{=}CH{-})]$ fragment as an electron donor[3] in candidates for SHG. The rationale being that theoretical[4] and experimental[5] research have demonstrated that electronic interaction between the $Fe_2\mu\text{-}C$ component and the conjugated system is maintained throughout rotation of the μ-C−vinyl bond.

Azulene displays many of the criteria essential for the exhibition of large first hyperpolarisabilities: it has an asymmetric charge distribution (azulene has a dipole moment of 0.8 D)[6] and it is noncentrosymmetric. Also unlike conventional organic donors such as *para*-(dialkylamino)phenyl substituents which lose resonance stabilisation upon charge separation, azulene and their alkylated derivatives are quite unique in that the disruption of aromaticity on going from the neutral to the charged form is counterbal-

---

[a] University College Dublin,
Belfield, Dublin 4, Ireland
E-mail: farrell@rz.uni-potsdam.de
Anthony.Manning@ucd.ie
[b] Institut für Anorganische und Angewandte Chemie, Universität Hamburg,
Martin-Luther-King-Platz 6, 20146 Hamburg, Germany
E-mail: heck@chemie.uni-hamburg.de
[c] Chemistry Dept., National University of Ireland,
Galway, Ireland

anced by the gain of resonance energy upon formation of the azulenylium carbocation, a 6π-electron aromatic tropylium analogue (Figure 1).[7] Thus, azulene appears to be an extremely novel and versatile system and it is surprising that there are very few reports to date of azulenic NLO chromophores.[7−10] The present study focuses on the synthesis and charcterisation of a novel series of organometallic merocyanines linking the [(CpFeCO)$_2$(μ-CO)(μ-C=CH−)] fragment to tropylium-based electron acceptors.

Figure 1. Resonance forms of a substituted azulenylium carbocation

Results and Discussion

Synthesis

Previous work revealed that the presence of the strong electron-donating dinuclear carbene reduces the reactivity of the formyl-substituted diiron complex [(CpFeCO)$_2$(μ-CO)(μ-C=CH−CHO)][11] (**1**) towards phosphorane nucleophiles but that extended μ-vinylidene complexes of the type [(CpFeCO)$_2$(μ-CO)(μ-C=CH−CH=CH−R)] are available using the more reactive Wittig−Horner−Wadsworth−Emmons (WHWE) reagents.[3] The diethyl (cycloheptatrienylmethyl)phosphonate (**2**) was prepared in a Michaelis−Arbuzov reaction from 1-chlormethyl-1,3,5-cycloheptatriene,[12] and treated with **1** in THF using *t*BuOK to yield the μ-vinylidene complex [(CpFeCO)$_2$(μ-CO)(μ-C=CH−CH=CH−C$_7$H$_7$)] (**3**) (Scheme 1). The trityl salt [Ph$_3$C][BF$_4$] was added to a solution of **3** in CH$_2$Cl$_2$ in order to abstract a hydride and to produce the tropylium derivative [(CpFeCO)$_2$(μ-CO)(μ-C=CH−CH=CH−C$_7$H$_6$)][BF$_4$]. A colour change from red-brown to blue was observed during the reaction and the IR spectrum of the reaction mixture showed the expected ν(CO) modes (2030, 1997, 1845 cm^{-1}), which are strongly shifted to higher energies compared to the corresponding ν(CO) modes of **3** (1996, 1960, 1795 cm^{-1}). However, the reaction mixture discoloured quickly and attempts to isolate the pure product were unsuccessful.

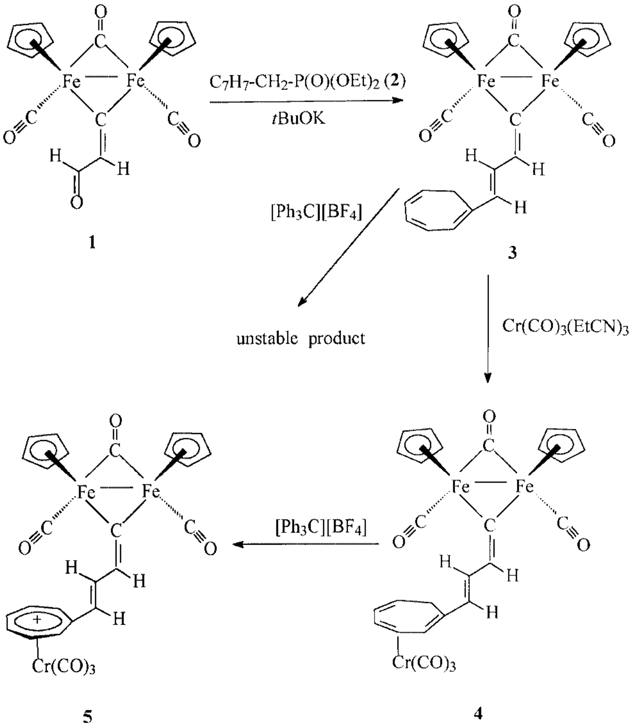

Scheme 1. Synthesis of the cationic dimetallic D−π−A complex **5**

It was expected that coordination of the Cr(CO)$_3$ fragment to the seven-membered ring would greatly enhance the stability of the tropylium derivative and this was achieved by first treating **3** with Cr(CO)$_3$(EtCN)$_3$ (Scheme 1) to generate the neutral heterometallic complex [(CpFeCO)$_2$(μ-CO){μ-C=CH−CH=CH−(η^6-C$_7$H$_7$)Cr(CO)$_3$}] (**4**) as a mixture of the isomers **4a** and **4b** (Figure 2). As before, the addition of the trityl cation to a solution of the complex **4** in CH$_2$Cl$_2$ was accompanied by a dramatic colour change from red-brown to deep blue indicating a strong enhancement in the electronic communication between the diiron terminus and the cationic tricarbonyl(tropylium)chromium moiety. By layering the reaction mixture with diethyl ether a microcrystalline solid was obtained which was characterised as the cationic heterometallic merocyanine [(CpFeCO)$_2$(μ-CO){μ-C=CH−CH=CH-(η^7-C$_7$H$_6$)Cr(CO)$_3$}][BF$_4$] (**5**).

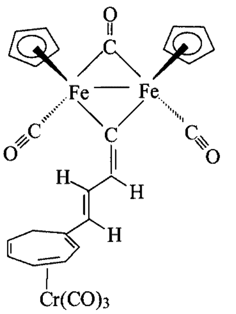

4a

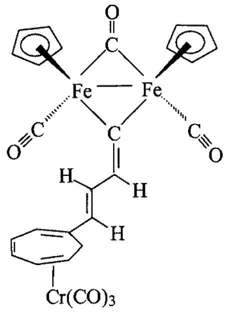

4b

Figure 2. Different diastereoisomers of the neutral complex **4**

The reaction of the μ-ethylidyne complex [(CpFeCO)$_2$(μ-CO)(μ-C−CH$_3$)][BF$_4$][13] (**6**) with aldehydes has been found to be a facile methodology towards the preparation of cationic diiron chromophores.[2] Nonetheless, purification problems have been experienced when longer reaction periods were necessary due to the formation of [CpFe(CO)$_3$][BF$_4$] which was extremely difficult to remove.[2a] Consequently, two complimentary procedures were attempted in order to isolate the organometallic azulenylium [{C$_{10}$H$_7$}]$^+$ and guaiazulenylium [{C$_{10}$H$_4$Me$_2$*i*Pr}]$^+$ merocyanines [(CpFeCO)$_2$(μ-CO)(μ-C=CH−CH={C$_{10}$H$_7$})][BF$_4$] (**7**) and [(CpFeCO)$_2$(μ-CO)(μ-C=CH−CH={C$_{10}$H$_4$Me$_2$*i*Pr})][BF$_4$] (**8**), and also to provide versatile access to a wide range of other vinyl−carbene/carbyne complexes. Azulene- and guaiazulene-1-carboxaldehyde[14] are readily available by literature procedures and these aldehydes were condensed with **6** in CH_2Cl_2 at 40 °C overnight giving intensely coloured reaction mixtures (Scheme 2). The air-stable merocyanine salts **7** and **8** were isolated upon filtering the reaction mixture and layering the filtrate with diethyl ether.

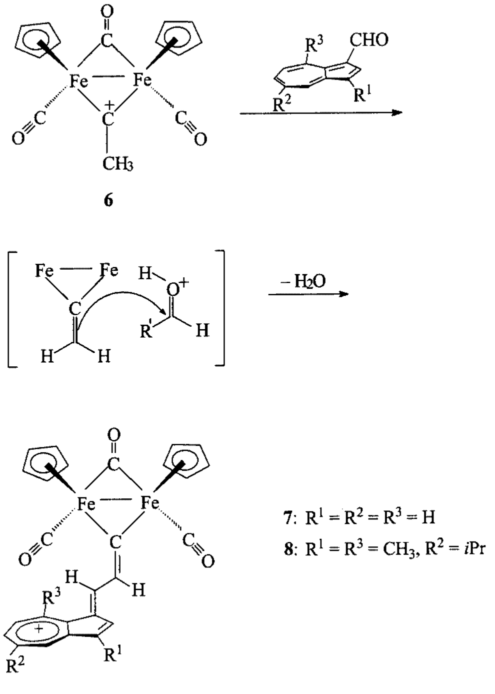

Scheme 2. Synthesis of the azulenylium and guaiazulenylium D−π−A complexes **7** and **8**

As organic[15] and organometallic[7] aldehydes have been found to react with azulenes under acidic conditions to form azulenylium based carbocationic complexes, an alternative synthetic route towards **7** and **8** was envisaged by the reaction of the formyl-substituted μ-vinylidene complex **1** with azulene and guaiazulene (Scheme 3). Condensation of **1** with an equimolar amount of azulene or guaiazulene in THF with a large excess of HBF_4 was indeed successful and again led to the isolation of **7** and **8** in high yields.

Crystal Structures of 3, 4 and 5

Crystal and structure refinement data for the X-ray analyses are presented in Table 1 and selected bond lengths and angles are listed in Table 2. Views of the molecular structures are illustrated in Figures 3−5 along with atom labelling. The $Fe_2(\eta\text{-}C_5H_5)(CO)_2(\mu\text{-}CO)(\mu\text{-}C)$ moiety has a *cis* structure while the π-linker displays an all-*trans* geometry in all of the structures. Of note is the similarity between the bond lengths across the all-$C_{sp2}-C_{sp2}$ π-bridge (C14−C17) in **3** and **4**, whereas **5** displays slightly shorter carbon−carbon single and elongated double bonds. This suggests a predominantly μ-carbene structure in **3** and **4** with little interaction between the diiron and cycloheptatriene moiety as depicted by the olefinic mesomeric form **I** in Figure 6. In **5** the alternation in the bond lengths of the π-bridge indicates an increased electronic interaction between the termini in the solid state, which can be rationalised as a distinct contribution of the vinylcarbyne mesomeric form **II** to the electronic ground state (GS).

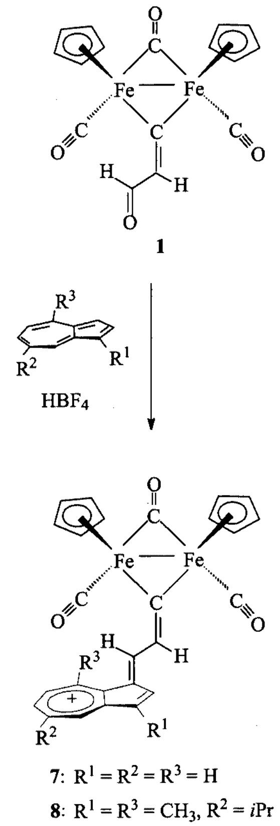

Scheme 3. Alternative synthetic route to **7** and **8**

The extent of the bond length alternation (BLA), which is defined as the difference between the average lengths of carbon−carbon single and double bonds, has been established as a useful indicator of high first hyperpolarisabilities.[16] Several attempts to relate β to both the molecular electronic and structural parameters led to the prediction that optimal NLO activity is achieved when BLA = 0.03−0.05 Å. The BLA across the π-bridge of complexes **3** and **4** is 0.10 Å and ca. 0.11 Å, respectively, whereas for **5** the BLA is 0.07 Å, which implies a medium first hyperpolarisability value for **5**.

Another notable feature of the X-ray diffraction study, which fortifies the evidence for the strong π-communication between the termini, especially in the case of the push-pull chromophore **5**, are the calculated dihedral angles. The larger angle between the planes made by $Fe_2\mu$-C and C14−C16 for **5** denotes a more flexible C14−C15 bond with a relatively lower bond order than for both **3** and **4**. Furthermore, the angle between the planes C14−C16 and C15−C17 increases in the order **5** < **4** < **3** (but are nonetheless quite low), attesting to the π-interaction of the entire conjugated linker.

Analysis of IR, ^{13}C and ^1H NMR spectra

One of the main considerations when characterising D−π−A-type compounds is the electronic configuration of

Table 1. Crystal data and structure refinement details for complexes **3**, **4** and **5**

	3	**4**	**5**
Formula	$C_{24}H_{20}Fe_2O_3$	$C_{27}H_{20}CrFe_2O_6$	$C_{28}H_{21}BCl_2CrF_4Fe_2O_6$
M_r	468.10	604.13	774.86
λ [pm]	7.1073	7.1073	7.1073
T [K]	153	153	293
Crystal system	triclinic	monoclinic	triclinic
Space group	$P\bar{1}$	$P2(1)/c$	$P\bar{1}$
a [Å]	8.7933(3)	7.305(4)	10.071(5)
b [Å]	9.5299(3)	27.261(16)	12.458(6)
c [Å]	12.7653(4)	12.163(7)	13.426(7)
α [°]	97.7220(10)	90	94.87(4)
β [°]	108.1740(10)	90.449	109.07(4)
γ [°]	90.500(10)	90	99.86(4)
V/ Å^3	1005.67(6)	2422(2)	1550.5(14)
Z	2	4	2
$\rho_{calcd.}$ [g cm^{-3}]	1.546	1.657	1.660
Abs. coeff. [mm^{-1}]	1.465	1.664	1.504
F(000)	480	1224	776
Crystal size [mm]	0.05 × 0.3 × 0.4	0.7 × 0.10 × 0.10	0.6 × 0.5 × 0.45
θ range [°]	2.44−30.00	1.49−25.03	2.46−27.5
Index range	$-12 \le h \le 12$	$-8 \le h \le 8$	$-1 \le h \le 13$
	$-13 \le k \le 13$	$-32 \le k \le 32$	$-16 \le k \le 15$
	$-17 \le l \le 17$	$-14 \le l \le 14$	$-17 \le l \le 16$
Total reflns.	25247	23460	7947
Unique reflns.	5789	4278	7112
Reflections [$I > 4\sigma(I)$]	5789	4278	7112
Parameters	244	326	407
GoF[a]	1.073	1.082	1.032
R_{int}	0.0372	0.1947	0.0326
$R1/wR2$ [$I > 2\sigma(I)$][b]	0.0384/0.1044	0.0857/0.1965	0.0524/0.1364
$R1/wR2$ (all data)[b]	0.0426/0.1069	0.1461/0.2314	0.0712/0.1531
Min./max. resd. [eA^{-3}]	−0.636/1.016	−1.010/0.853	−0.510/0.681

[a] GoF = $[\Sigma w(F_o^2 - F_c^2)^2/(n - p)]^{1/2}$; n = numbers of reflections, p = numbers of parameters. [b] $R1 = (\Sigma||Fo| - |Fc||)/\Sigma|Fo|$, $wR2 = [\Sigma w(F_o^2 - F_c^2)^2]/\Sigma w(F_o^2)^2]^{1/2}$.

Table 2. Selected bond lengths [Å] and angles [°] for **3**, **4** and **5**

Bond Lengths	**3**	**4**	**5**
C(1)−O(1)	1.173(2)	1.199(15)	1.137(5)
C(2)−O(2)	1.142(2)	1.142(17)	1.142(5)
C(3)−O(3)	1.136(2)	1.119(15)	1.181(5)
C(14)−C(15)	1.339(2)	1.332(18)	1.350(5)
C(15)−C(16)	1.449(2)	1.447(18)	1.423(5)
C(16)−C(17)	1.353(2)	1.341(17)	1.360(5)
C(17)−C(18)	1.452(2)	1.437(17)	1.439(5)
C(18)−C(19)	1.508(2)	1.520(17)	1.418(5)
C(18)−C(24)	1.363(2)	1.375(17)	1.431(5)
C(19)−C(20)	1.508(2)	1.486(17)	1.399(6)
C(20)−C(21)	1.331(3)	1.382(18)	1.406(7)
C(21)−C(22)	1.448(3)	1.416(19)	1.384(7)
C(22)−C(23)	1.345(3)	1.375(19)	1.413(6)
C(23)−C(24)	1.442(2)	1.408(19)	1.390(5)
Dihedral angles			
[Fe(1)−C(14)−Fe(2)][C(14)−C(16)][a]	3.7(3)	2.2(1)	−4.6(4)
[C(14)−C(16)][C(15)−C(17)][a]	12.3(4)	9.6(2)	2.4(5)
[C(15)−C(17)][C(16)−C(18)][a]	6.0(4)	0.8(2)	3.0(5)

[a] Angle between the two planes.

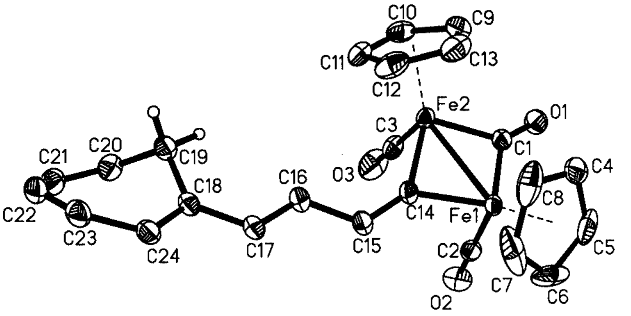

Figure 3. Molecular structure of **3** (30% ellipsoids; the hydrogen atoms are omitted for clarity except for C19, which is the C_7H_7 sp^3-carbon atom)

the molecules and how this affects the properties of the material. The systematic modification of a system coupled with the detailed analysis of the resulting changes may allow us to formulate a relationship between the molecular structure and the properties. This would greatly enhance our ability to tune a system structurally in order to maximise a particular output. In the case of these μ-vinylidene complexes the GS electronic constitution is easily evaluated by considering (i) the carbonyl stretching frequencies,

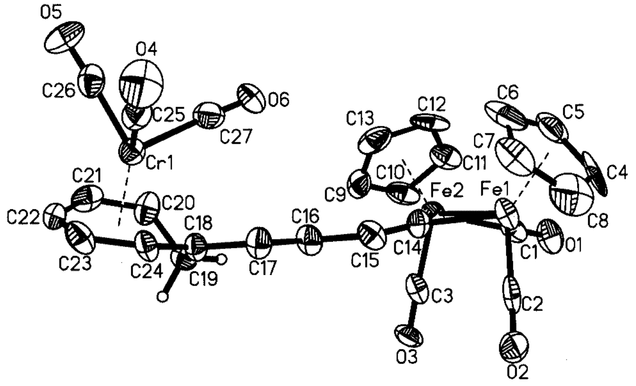

Figure 4. Molecular structure of **4** (30% ellipsoids; the hydrogen atoms are omitted for clarity except for C19, which is the C_7H_7 sp^3-carbon atom)

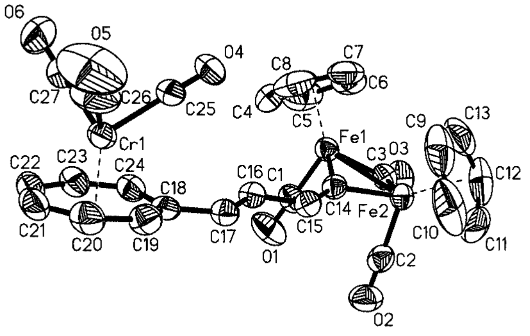

Figure 5. Molecular structure of **5** (30% ellipsoids; hydrogen atoms and the BF_4^- counterion are omitted for clarity)

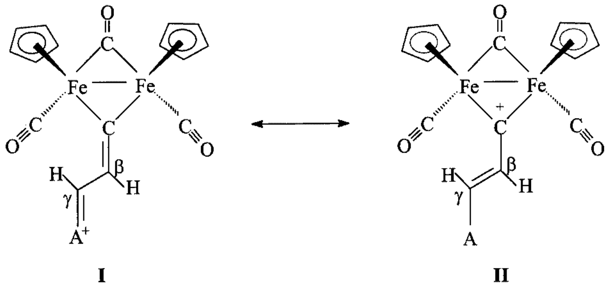

I **II**

Figure 6. Mesomeric forms of the cationic donor−acceptor complexes $[(CpFeCO)_2(\mu\text{-}CO)(\mu\text{-}C{=}CH{-}CH{=}A^+)]$ where A^+ = $[CH{-}(\eta^7\text{-}C_7H_6)Cr(CO)_3]^+$ (**5**), $[C_{10}H_7]^+$ (azulenylium) (**7**), $[C_{10}H_4Me_2\textit{i}Pr]^+$ (guaiazulenylium) (**8**)

(ii) the number of Cp signals in both the ^1H and ^{13}C NMR spectra, (iii) the ^1H-^1H coupling constants across the unsaturated bridging ligand, and (iv) the chemical shift of the μ-carbon signal in the ^{13}C NMR spectra.

The solution IR spectra of all the complexes prepared reveal one bridging and two terminal carbonyl stretching modes, the relative intensities of which are consistent with a *cis* arrangement of these CO ligands. The wavenumbers of these ν(CO) bands are very informative in determining the extent of electronic coupling between the $Fe_2\mu\text{-}C{=}CH$- and the tropylium-based termini (Table 3). A predominant μ-vinylidene resonance contribution to the GS (**I**, Figure 6), can be concluded from ν(CO) bands at lower wavenumbers [ν(CO): ca. 1992, 1953 cm^{-1}].[3,17] On the other hand, charge delocalisation throughout the molecule due to increased contribution from the mesomeric form **II** to the GS (Figure 6), decreases the electron density at the $Fe_2\mu$-C core reducing the degree of M→CO back donation. The resulting ν(CO) shift to higher wavenumbers tends towards that of **6** [ν(CO): 2046, 2000 cm^{-1}][2,18] where the positive charge is fully localised on the diiron end group. As expected, the neutral fragment $[(\eta^6\text{-}C_7H_7)Cr(CO)_3]$ is the weakest electron acceptor with ν(CO) bands at 1997, 1961 cm^{-1}, followed by the corresponding cation $[(\eta^7\text{-}C_7H_6)Cr(CO)_3]^+$ with the CO stretching modes at 2007 and 1975 cm^{-1}. As expected, the azulenylium-type end groups are stronger electron acceptors due to the resonance stabilisation in both extreme mesomeric forms and display increased contribution from the μ-vinyl−carbyne resonance forms **II** to the overall GS structure. Alkylation of the azulenylium moiety results in a more stable carbocation and a weaker electron acceptor with the result that the azulenylium complex **7** exhibits the highest ν(CO) modes.

Table 3. IR, ^1H and ^{13}C NMR spectroscopic data for the complexes $[(CpFeCO)_2(\mu\text{-}CO)(\mu\text{-}C{=}CH{-}A)]$

Acceptor		IR (cm^{-1})[a]			^1H NMR (Hz)	^{13}C NMR (ppm)
A		ν(CO)		ν(μ-CO)	$J(H_\beta\text{-}H_\gamma)$	μ-C
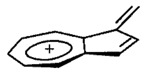	(**7**)	2024	1993	1832	13.5[b]	395[b]
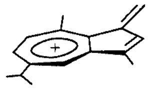	(**8**)	2017	1990	1829	12.6[b]	382[b]
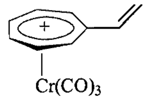	(**5**)	2007	1975(sh)	1812	11.0[b]	324[b]
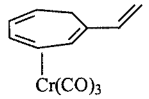	(**4**)	1997	1961	1796	10.3[c]	292[c]
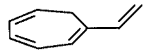	(**3**)	1996	1960	1795	10.1[c]	288[c]

[a] Solvent CH_2Cl_2. [b] Solvent $(CD_3)_2CO$. [c] Solvent $CDCl_3$.

An excellent diagnostic of the degree of charge delocalisation is the chemical shift of the μ_2-carbon atom of the π-bridge between the donor and acceptor in the ^{13}C NMR spectra (Table 3).[2,3] Increasing the potency of the electron acceptor augments the electronic interaction between the termini and the contribution from the (vinylcarbyne)diiron mesomeric form **II**. The reduction of electron density at the diiron framework results in the bridging carbon signal occurring at lower field strengths. From the position of these μ-C signals we can conclude that the azulenylium carbocations are by far the strongest electron acceptors within the presented series.

Comparing the ^1H-^1H coupling constants across the bridging $C_\beta{-}C_\gamma$ (Figure 6) bond should also aid in elucidating the GS electronic arrangement with $J(^1H_\beta\text{-}^1H_\gamma)$ increasing as the bond order increases (Table 3). Considering the limiting mesomeric form **I** (Figure 6), which contains an sp^2-carbon−sp^2-carbon single bond between C_β and C_γ, $^1H_\beta$-$^1H_\gamma$ coupling constants of about 10 Hz are to be expected.[3,19] For **3** and **4** the structural data are in agreement with a C_β−C_γ localised carbon−carbon single bond and the neutral "true" μ-vinylidene compound **3** exhibits the lowest coupling constant at $J = 10.1$ Hz. For compound **4** the $^1H_\beta$-$^1H_\gamma$ coupling value is slightly larger and the μ-^{13}C nucleus is deshielded to a smaller extent compared to **3**, demonstrating a small increase in the electron-withdrawing capability of the cycloheptatriene moiety due to the $Cr(CO)_3$ coordination. Consequently, the C_α−C_β bond remains predominantly a carbon−carbon double bond with a restricted rotation about the μ-C=CH bond. Hence, the Cp and terminal CO ligands are formally in different environments, and **3** as well as **4** exhibit two Cp and two CO signals in the ^{1}H and ^{13}C NMR spectra, respectively. When the bond order between C_β and C_γ displays increased C−C double bond character, as occurs in (μ-vinylcarbyne)diiron cations (mesomeric form **II** in Figure 6), the $^1H_\beta$-$^1H_\gamma$ coupling constants increase to 14.9 Hz and only one Cp and CO signal appear in the NMR spectra.[2]

The increase in $J(^1H_\beta$-$^1H_\gamma)$ agrees with the general downfield shift of the μ-C_α resonance signal of the diiron moiety and a graphic displays a linear correlation between δ(μ-^{13}C) and $J(^1H_\beta$-$^1H_\gamma)$ (Figure 7). These results present strong indications that in solution there exists an increasing charge delocalisation in the order **3** < **4** << **5** << **8** < **7** for the electronic ground state, which concurs with the ordering of electron-accepting strength from the IR data. It is noteworthy that only one Cp and one CO signal are observed in the NMR spectra for all of the cationic chromophores. This is in accordance with the structural data of **5**, which displays a marked decrease of the μ-C_α−C_β double-bond character and increase of C_β−C_γ bond order in the solid state. This effect may be augmented by the ion-pair separation in solution whereas in the solid state the inter ion-pair Coulomb interaction will diminish the D−A interaction within the entire cation. The correlation between δ(μ-^{13}C) and $J(H_\beta$-$H_\gamma)$ indicates a considerable contribution of the μ-vinylcarbyne mesomeric form **II** to the electronic ground states for **7** and **8** in solution, which even dominates for **7**. Hence, the diiron derivatives under study represent a rare example of organometallic D−π−A complexes wherein the electronic ground state can be varied from an organometallic merocyanine-type species, in which the positive charge is mainly localised on the seven-membered ring moiety as in **5**, to a merocyanine wherein the positive charge is mainly localised on the diiron terminus as in **7**. A suitable selection of the cationic acceptor would enable the development of an organometallic polymethine with a complete delocalisation of the positive charge.

Electronic Absorption Spectra

A commonly used model called the two-level approximation relates β to the molecular optical properties and predicts that large first hyperpolarisabilities are favoured by molecules possessing intense, low-energy and highly solvatochromic charge transfer (CT) transitions.[20] These fundamental parameters cannot be optimised independently and may not be weighted equally for a particular system. For example, for the series of compounds $[(CpFeCO)_2(\mu\text{-}CO)(\mu\text{-}C{-}\{\pi\text{-bridge}\}{-}Fc)][BF_4]$[2b] (Fc = ferrocenyl) it was found that a large solvatochromic shift and extinction coefficient upon photoexcitation were more important to the enhancement of β than the energy of the transition.

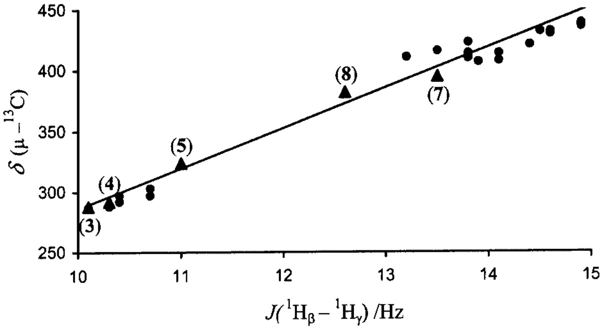

Figure 7. Correlation between δ(^{13}C) of the μ-C atom and the *J* coupling constants between H_β and H_γ of the π-bridge (●: data points from refs.[2,3])

The optical absorption data for the chromophores are presented in Table 4. The electronic spectra of the merocyanine salts display an intense asymmetric absorption in the visible region between 570 and 635 nm indicating a superimposition of different transitions. The two azulenylium chromophores also reveal a much weaker transition at lower energies (Figure 8). We assign the stronger absorption band to a donor−acceptor charge-transfer (DACT) transition and propose that the lower energy band is an azulene-localised π−π* transition. The strong electronic transitions are governed by medium negative solvatochromism which points towards a slightly more charge delocalised photoexcited state. However, the negative solvatochromism is much smaller than that observed for other cationic diiron NLO chromophores,[2a] confirming a certain degree of charge delocalisation in the electronic ground state as already concluded from the NMR results. This finding is also corroborated in that the solvatochromism and thus dipole change Δμ between the ground and the excited state decreases with increasing charge delocalisation: **5** > **8** > **7**. Also of note is that increasing the electron-accepting capabilities of the tropylium-based termini results in a blue shift to the CT bands (Figure 9). This is consistent with an energetically lower lying molecular orbital being involved in the CT transition as a consequence of higher GS charge delocalisation.

Hyperpolarisability Measurements

The complexes **5**, **7** and **8** were subjected to hyper-Rayleigh scattering (HRS) studies[21] but as they absorb substantially in the area of 532 nm [i.e. $I(2\omega)$ when the incident light has a wavelength of $I(\omega) = 1064$ nm], the stimulating laser light was shifted to a higher wavelength (1500 nm). Thus, the superposition of a strong absorption and the HRS signal is minimised, which makes the calculated static

Table 4. Linear and nonlinear optical data of the complexes for the complexes [$(CpFeCO)_2(\mu\text{-}CO)(\mu\text{-}C{=}CH{-}A)$]

Acceptor		λ_{max} (ε) [nm (M^{-1} cm^{-1})][a] CH_2Cl_2	CH_3CN	$\Delta\tilde{\nu}$[b] (cm^{-1})	β[a] (10^{-30} esu)	β_0 (10^{-30} esu)
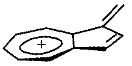	**(7)**	579 (55621)	571 (41437)	–242	nd[d]	–
		732 (1240)	721 (1651)	–208		
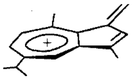	**(8)**	608 (62569)	599 (53877)	–247	274	79
		771 (2287)	756 (1412)	–257		
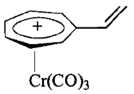	**(5)**	635 (67211)	625 (67389)	–252	451	117
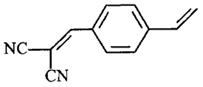	**(9)**[c]	523 (34450)	509 (29100)	–526	156	68
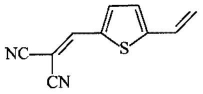	**(10)**[c]	565 (29590)	556 (33280)	–286	227	84

[a] Measured in CH_2Cl_2 solution at λ = 1500 nm, using DR1 as standard: $\beta(DR1, CH_2Cl_2) = 70 \times 10^{-30}$ esu. [b] $\Delta\tilde{\nu} = \tilde{\nu}_{max}(CH_2Cl_2) - \tilde{\nu}_{max}(CH_3CN)$. [c] Taken from ref.[3] [d] nd: not detected.

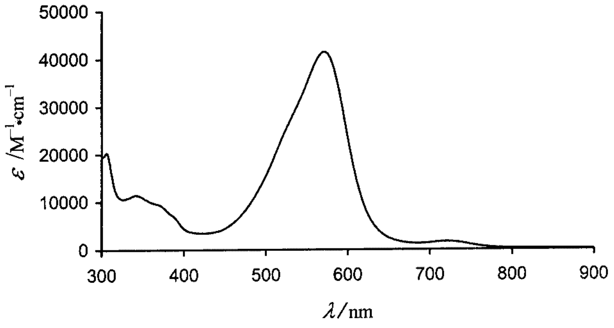

Figure 8. Electronic absorption spectra of **7** in CH_3CN

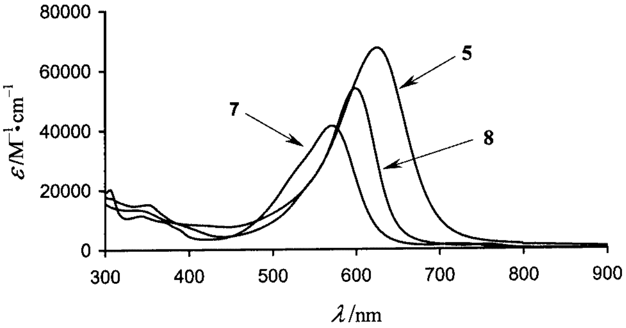

Figure 9. Electronic absorption spectra of **5**, **7** and **8** in CH_3CN

hyperpolarisability (β_0)[20] more reliable.[22,23] Another important reason for using the higher wavelength incident beam, is an attempt to discriminate between a true SHG signal and a two-photon absorption-induced fluorescence (TPAF) enhanced signal[24–26] The 1500-nm incident-beam HRS examinations were achieved using a tuneable optical parametric oscillator (OPO) based set-up.[23] All measurements were carried out using Desperse Red 1 (DR1) as an external standard. The reference hyperpolarisability β of DR1 in CH_2Cl_2 was calculated by comparing the slopes of the standard in CH_2Cl_2 and $CHCl_3$ to obtain the ratio of β_{solute}.[27] Using the value $\beta(CHCl_3) = 80 \times 10^{-30}$ esu[24] the hyperpolarisability of DR1 in CH_2Cl_2 is estimated to be 70×10^{-30} esu. The effect of the refractive indices of the solvents was corrected using the simple Lorentz local field.[28]

The first hyperpolarisability β could only be obtained for the cationic dimetallic complex **5** (451×10^{-30} esu) and the guaiazulenylium derivative **8** (274×10^{-30} esu) (Table 4), complex **7** did not show any intensity in the HRS experiment. The obtained β values are in the order of magnitude of β values found for the neutral diiron donor-based complexes containing dicyanovinyl-substituted arenes as electron acceptors ($\beta = 156 \times 10^{-30}$ esu and $\beta = 227 \times 10^{-30}$ esu, Table 4).[3] The very low extinction coefficients for the complexes **5** and **8** at λ = 750 nm allows a reliable calculation of the static hyperpolarizability β_0 using the two-level model[20b] [$\beta_0(\mathbf{5}) = 117 \times 10^{-30}$ esu and $\beta_0(\mathbf{8}) = 79 \times 10^{-30}$ esu]. It is noteworthy that the static hyperpolarisabilities of the four diiron donor-based NLO chromophores in Table 4 can be correlated with $J(H_\beta\text{-}H_\gamma)$, which is a measure of the carbon–carbon bond order between C_β and C_γ (vide supra) and thus, synonymous to the carbon–carbon bond length (Figure 10). The β_0 values improve with increasing $J(H_\beta\text{-}H_\gamma)$ values beyond 11 Hz and then decreases distinctly for $J(H_\beta\text{-}H_\gamma)$ = 12.6 Hz for **8**, and for complex **7** with $J(H_\beta\text{-}H_\gamma)$ = 13.5 Hz the first hyperpolarisability even vanishes. This behaviour very much resembles the correlation between the static hyperpolarizability β_0 and the bond-length alternation (BLA) in donor–acceptor-substituted polyenes found by Marder et al.[16] Therefore, the small β_0 value for **8** may be explained by the smaller BLA due to the large contribution of the μ-vinylcarbyne mesomeric form **II** to the ground state. Since the X-ray data demonstrate that in the solid state the BLA for **5** is still beyond the optimum value of 0.03–0.05, we suggest that a maximum of the β_0 values in the diiron-based NLO chromophores may be obtained, when the accepting capability of the seven-membered ring moiety is slightly enhanced compared to the [$(\eta^7\text{-}C_7H_6)Cr(CO)_3$]$^+$ acceptor but less potent than for the guiazulenylium or even azulenylium electron acceptors.

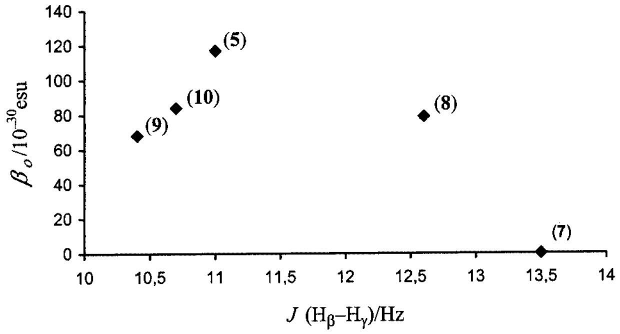

Figure 10. Correlation between the first static hyperpolarisability β_0 and the coupling constants $J(H_\beta\text{-}H_\gamma)$

The NLO properties of a series of organometallic merocyanines utilising the [$(CpFeCO)_2(\mu\text{-}CO)(\mu\text{-}C{=}CH{-})$] fragment as an electron donor linked to thiobarbituric acid by olefinic units, demonstrated the effectiveness of the diiron unit.[27] The second-order optical nonlinearities were determined using electric-field-induced second harmonic generation (EFISH). However, as there exist problems in comparing results obtained from different techniques[25,26] no correlations will be attempted. Static hyperpolarisabilities from 1500-nm HRS experiments have been reported for organic 1D, 2D and 3D NLO chromophores.[27,28] An extremely large β_0 value was reported for the 2D NLO truxenone derivative ($\beta_0 = 169 \times 10^{-30}$ esu)[29] which is still larger than the value of β_0(**5**). However, in terms of their static hyperpolarisability to molecular mass ratio β_0/M, which is often used as a figure of merit, values of β_0/M(**5**) $= 0.153 \times 10^{-30}$ ($esu{\cdot}mol^{-1}{\cdot}g^{-1}$) and β_0/M(**8**) $= 0.149 \times 10^{-30}$ ($esu{\cdot}mol^{-1}{\cdot}g^{-1}$) were calculated for the present organometallic merocyanines, which compare well with the corresponding value of the truxenone chromophore $\beta_0/M = 0.124 \times 10^{-30}$ ($esu{\cdot}mol^{-1}{\cdot}g^{-1}$).

Conclusion

The facile synthesis is presented for a series organometallic merocyanines based on the diiron moiety [$(CpFeCO)_2(\mu\text{-}CO)(\mu\text{-}C{=}CH{-})$] as the electron donor and the cationic tropylium derivatives [$-C{=}CH(\eta^7\text{-}C_7H_6)Cr(CO)_3$]$^+$ and azulenylium and guaiazulenylium as electron-accepting units, which tune the electronic properties of these D−A complexes. In ^{13}C NMR spectroscopic studies an increased deshielding of the μ-C atom of the π-bridge is observed in the order **5** < **8** < **7**, thus demonstrating the increased electron-accepting capability of the cationic seven-membered ring units in that order. Additionally, a correlation between δ(μ-^{13}C) and $J(H_\beta\text{-}H_\gamma)$ is found which indicates a slightly stronger contribution of the μ-vinylcarbyne mesomeric form **II** to the ground state in solution for the azulenylium and guaiazulenylium congeners **7** and **8**, whereas for the tropylium derivative **5** the ground state displays extensive contribution from the μ-vinylidene mesomeric form **I**. The cationic complexes reveal a strong absorption band in UV/Vis spectra around 600 nm due to a DA−CT transition, which undergoes a medium negative solvatochromic shift. The analysis of the nonlinear optical properties by means of HRS measurements was successful for **5** and **8** and reveals that the combination of the diiron donor and the tricarbonyl(η^7-tropylium)chromium cation provides the larger experimental and static first hyperpolarisabilities β and β_0, respectively. A correlation between $J(H_\beta\text{-}H_\gamma)$ and the static hyperpolarisability β_0 very much resembles the dependence of β_0 on the bond length alternation (BLA). Hence, although the guaiazulenylium cation is a considerably stronger electron acceptor, the smaller β_0 value of **8** may be explained by a smaller bond length alternation due to the larger contribution of the μ-vinylcarbyne mesomeric form **II**.

Experimental Section

Solvent Purification and Instrumentation: Dichloromethane, diethyl ether and THF were dried by refluxing in the presence of calcium hydride and distillation prior to use. THF was further distilled from sodium/benzophenone. Infrared spectra were recorded with a Perkin−Elmer Paragon 1000 spectrometer. UV/Vis spectra were recorded with a Perkin−Elmer Lambda 6 spectrometer and a Perkin−Elmer model 554. NMR spectra were recorded with JEOL JNM-GX 270 FT and Varian Gemini 200 BB spectrometers using TMS as an internal standard. Elemental analyses were carried out by the Microanalytical Laboratory, University College, Dublin and the Institut für Anorganische und Angewandte Chemie, Universität Hamburg.

[$(CpFeCO)_2(\mu\text{-}CO)(\mu\text{-}C{=}CH{-}CH{=}CH{-}C_7H_7)$] (3): *t*BuOK (0.13 g, 1.16 mmol) was added to a solution of [$(CpFeCO)_2(\mu\text{-}CO)(\mu\text{-}C{=}CH{-}CHO)$][11] (**1**) (0.3 g, 0.79 mmol) and diethyl (cycloheptatrienylmethyl)phosphonate (**2**)[12] (1.1 equiv.) in dry THF (50 mL). Stirring was continued for 1 h under nitrogen, water (30 mL) was added and the mixture was extracted with dichloromethane. The organic layer was dried with $MgSO_4$ and the solvent was removed. The residue was taken up in dichloromethane and chromatographed on alumina. Product **3** eluted with dichloromethane and was recrystallised from CH_2Cl_2/hexane. Yield: 0.30 g (82%). ^1H NMR ($CDCl_3$): δ = 8.17 (d, *J* = 10.1 Hz, 1 H, μ-C=C*H*), 7.03 (dd, *J* = 10.1, 15.2 Hz, 1 H, μ-C=CH−C*H*), 6.62 (m, 1 H, C_7H_7), 6.46 (m, 1 H, C_7H_7), 6.20 (m, 3 H, μ-C=CH−CH=C*H*, C_7H_7), 5.44 (m, 1 H, C_7H_7), 4.90 (s, C_5H_5), 4.81 (s, C_5H_5), 2.74 (m, 2 H, C_7H_7) ppm. $^{13}C\{^1H\}$ NMR ($CDCl_3$): δ = 288.3 (μ-C), 270.8 (μ-CO), 210.7, 210.6 (CO), 144.3, 132.8 124.9 (μ-C=CH−CH=CH), 134.0 (C_q, C_7H_7), 131.6, 129.3, 128.1, 124.2, 122.1 (C_7H_7), 88.4, 87.8 (C_5H_5), 29.1 (C_7H_7) ppm. IR (CH_2Cl_2): $\tilde{\nu}$ = 1996 (vs), 1960 (m) [ν(CO)]; 1795 (s) [ν(μ-CO)]; 1607 (m), 1558 (w) [ν(C=C)] cm^{-1}. $C_{24}H_{20}Fe_2O_3$ (468.10): calcd. C 61.58, H 4.31; found C 61.04, H 4.68.

[$(CpFeCO)_2(\mu\text{-}CO)\{\mu\text{-}C{=}CH{-}CH{=}CH{-}(\eta^6\text{-}C_7H_7)Cr(CO)_3\}$] (4): Compound **3** (0.3 g, 0.64 mmol) and $Cr(CO)_3(EtCN)_3$[29] (0.19 g, 0.63 mmol) were stirred in dry THF (40 mL) overnight under N_2. The solvent was removed and the residue taken up in the minimum volume of dichloromethane and chromatographed on alumina. The column was washed with toluene to remove traces of unreacted **3**. Product **4** eluted with dichloromethane and was recrystallised from CH_2Cl_2/hexane. Yield: 0.28 g (73%). ^1H NMR ($CDCl_3$, only one isomer given): δ = 8.21 (d, *J* = 10.3 Hz, 1 H, μ-C=C*H*), 6.86 (dd, *J* = 10.4, 15.0 Hz, 1 H, μ-C=CH−C*H*), 5.89 (m, 2 H, η^6-C_7H_7), 5.74 (d, *J* = 15.2 Hz, 1 H, μ-C=CH−CH=C*H*), 5.13 (m, 1 H, η^6-C_7H_7), 4.96 (s, C_5H_5), 4.86 (s, C_5H_5), 4.85 (hidden, 2 H, η^6-C_7H_7), 3.35 (m, 2 H, η^6-C_7H_7) ppm. $^{13}C\{^1H\}$ NMR ($CDCl_3$): δ = 292.1 (μ-C), 269.6 (μ-CO), 232.6 [$Cr(CO)_3$], 209.9, 209.8 (CO), 143.3, 134.1 123.3 (μ-C=CH−CH=CH), 100.7, 98.0, 97.6, 96.8, 96.3 (η^6-C_7H_7), 88.0, 87.5 (C_5H_5), 23.7 (η^6-C_7H_7) ppm. IR (CH_2Cl_2): $\tilde{\nu}$ = 1997 (vs), 1961 (m), 1898 (vs), 1869 (s) [ν(CO)]; 1796 (s) [ν(μ-CO)]; 1607 (m), 1558 (w) [ν(C=C)] cm^{-1}. $C_{27}H_{20}CrFe_2O_6$ (604.13): calcd. C 53.68, H 3.34; found C 53.09, H 3.60.

[$(CpFeCO)_2(\mu\text{-}CO)\{\mu\text{-}C{=}CH{-}CH{=}CH{-}(\eta^7\text{-}C_7H_6)Cr(CO)_3\}$][$BF_4$] (5): [$Ph_3C$][$BF_4$] (0.10 g, 0.30 mmol) was added to a solution of **4** (0.2 g, 0.33 mmol) in dry CH_2Cl_2 (50 mL) at −70 °C. The reaction mixture was allowed to warm to room temperature and then filtered. Product **5** was obtained by layering the filtrate with dry diethyl ether (50 mL) and cooling overnight. Yield: 0.16 g (70%). ^1H NMR [$(CD_3)_2CO$]: δ = 8.69 (d, *J* = 11.0 Hz, 1 H, μ-

C=C*H*), 8.04 (dd, J = 11.0, 14.6 Hz, 1 H, μ-C=CH−C*H*), 6.95 (m, 2 H, η^7-C_7H_6), 6.70 (m, 4 H, η^7-C_7H_6), 6.39 (d, 1 H, μ-C=CH−CH=C*H*), 5.22 (s, 10 H, C_5H_5). $^{13}C\{^1H\}$ NMR [$(CD_3)_2CO$]: δ = 323.7 (μ-C), 265.6 (μ-CO), 225.1, [$Cr(CO)_3$], 211.6 (CO), 146.9, 145.7 116.5 (μ-C=CH−CH=CH), 135.3 (C_q, η^7-C_7H_6), 106.0, 103.5, 98.4 (η^7-C_7H_6), 89.8 (C_5H_5) ppm. IR (CH_2Cl_2): $\tilde{\nu}$ = 2043 (s), 2007 (vs), 1970 (sh) [ν(CO)]; 1812 (m) [ν(μ-CO)]; 1606 (w), 1562 (m), 1468 (vs), 1456 (s) [ν(C=C)] cm^{-1}. $C_{27}H_{19}BCrF_4Fe_2O_6\cdot CH_2Cl_2$ (774.86): calcd. C 43.36, H 2.71; found C 43.63, H 2.67.

General Procedure for the Condensation of Azulenic Aldehydes with [$(CpFeCO)_2$(μ-CO)(μ-C−CH_3)][BF_4] (6): Complex **6** (0.25 g, 0.57 mmol) and an excess of aldehyde (1.2 equiv.) were stirred in CH_2Cl_2 (50 mL) at 35 °C for 12 h. The reaction mixture was filtered and the product precipitated from the filtrate by carefully adding diethyl ether (25 mL) and cooling overnight.

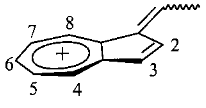

[$(CpFeCO)_2$(μ-CO)(μ-C=CH−CH={$C_{10}H_7$})][BF_4] (7): Yield: 0.23 g (70%). ^1H NMR ($CDCl_3$): δ = 9.88 (d, J = 13.5 Hz, 1 H, μ-C−C*H*=CH), 9.24 (d, J = 9.6 Hz, 1 H, 4-H), 8.74 (d, J = 9.9 Hz, 1 H, 8-H), 8.71 (d, J = 4.2 Hz, 1 H, 2-H), 8.38 (d, J = 13.5 Hz, 1 H, μ-C−CH=C*H*), 8.23 (t, J = 9.6 Hz, 1 H, 6-H) 8.02 (m, 2 H, 5-H, 7-H), 7.77 (d, 1 H, J = 4.22 Hz, 3-H), 5.34 (s, 10 H, C_5H_5) ppm. $^{13}C\{^1H\}$ NMR (CD_3CN): δ = 394.5 (μ-C), 258.9 (μ-CO), 209.5 (CO), 149.1, 146.2 (μ-C−CH=CH), 152.2, 148.7, 127.1 (C_q, $C_{10}H_7$), 143.9, 141.5, 138.5, 135.2, 134.0, 127.3 ($C_{10}H_7$), 91.1 (C_5H_5) ppm. IR (CH_2Cl_2): $\tilde{\nu}$ = 2024 (vs), 1993 (m) [ν(CO)]; 1832 (s) [ν(μ-CO)]; 1605 (m), 1546 (m), 1518 (vs), 1464 (m) [ν(C=C)] cm^{-1}. $C_{26}H_{19}BF_4Fe_2O_3$ (577.92): C 53.98, H 3.29; found C 54.19, H 3.62.

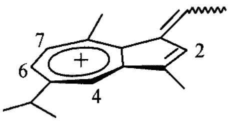

[$(CpFeCO)_2$(μ-CO)(μ-C=CH−CH={$C_{10}H_4Me_2$*i*Pr})][BF_4] (8): Yield: 0.29 g (80%). ^1H NMR ($CDCl_3$): δ = 9.66 (d, J = 12.6 Hz, 1 H, μ-C−C*H*=CH), 8.61 (d, J = 12.6 Hz, 1 H, μ-C−CH=C*H*), 8.50 (s, 1 H, 2-H), 8.44 (s, 1 H, 8-H), 8. (m, 2 H, 6-H, 7-H), 5.26 (s, 10 H, C_5H_5), 3.4 [m, 1 H, CH, *i*Pr], 3.34 (s, 3 H, CH_3), 2.65 (s, 3 H, CH_3), 1.42 [d, 1 H, J = 7.03 Hz, $(CH_3)_2$, *i*Pr]. $^{13}C\{^1H\}$ NMR (CD_3CN): δ = 382.0 (μ-C), 259.8 (μ-CO), 209.7 (CO), 152.7, 148.9 (μ-C−CH=CH), 153.6, 151.2, 150.4, 144.8, 142.2, 129.3 (C_q, $C_{10}H_4Me_2$*i*Pr), 140.6, 139.9, 136.7, 135.9 ($C_{10}H_4Me_2$*i*Pr), 90.4 (C_5H_5), 39.2, 13.8 (CH_3), 29.7 (CH, *i*Pr), 24.7 [$(CH_3)_2$, *i*Pr] ppm. IR (CH_2Cl_2): $\tilde{\nu}$ = 2017 (vs), 1990 (m) [ν(CO)]; 1829 (s) [ν(μ-CO)]; 1605 (m), 1552 (m), 1534 (s), 1501 (s) [ν(C=C)] cm^{-1}. $C_{31}H_{29}BF_4Fe_2O_3$ (648.05): C 57.45, H 4.51; found C 57.81, H 4.90.

Reaction of azulene and guaiazulene with [$(CpFeCO)_2$(μ-CO)(μ-C=CH−CHO)] (1): An excess of HBF_4 (54% solution in diethyl ether) was added to an equimolar solution of azulene or guaiazulene and **1** (0.25 g, 0.57 mmol) in dichloromethane (50 mL). The reaction mixture was concentrated until a colour change occurred and then stirred for 2 h. The products were precipitated from the solution by adding diethyl ether (75 mL) and cooling overnight. The resulting precipitates were filtered off and washed well with diethyl ether. The yields were 0.28 g (85%) of **7** and 0.30 g (83%) of **8**.

X-ray Structure Determination: Crystals suitable for an X-ray structure analysis were obtained by diffusion of Et_2O into a CH_2Cl_2 solution of **5** and by layering a CH_2Cl_2 solution of **3** and **4**, respectively with hexane. Complex **5** crystallises with three independent molecules of CH_2Cl_2. The data for structures **3** and **4** were obtained with a Bruker SMART-APEX diffractometer with an Mo-K_α X-ray tube as radiation source. The data for the structure of **5** was collected on a four-circle diffractometer Hilger & Watts, Mo-K_α, λ = 0.71073 Å. Complex **4** crystallises as a merohedral twin with two perpendicular monoclinic unit cells (with opposite oriented z axes) leading to a nearly orthorhombic cell. Symmetry-absence conditions did not give any suitable orthorhombic space group. The structure was solved and refined as a twin in the monoclinic space group $P2_{1/c}$ with β = 90.449°. Refinement in the same space group without the TWIN option leads to an R_1 value above 19% and worse standard deviations for geometric parameters. All structures were resolved by direct methods (SHELXL-86).[30] Refinement on F^2 was carried out by full-matrix least-squares techniques (SHELXL-93, SHELXL-97).[31,32] All non-hydrogen atoms were refined with anisotropic thermal parameters. The hydrogen atoms were refined by the riding-model method with a fixed isotropic thermal parameter related by a factor of 1.2 to the value of the equivalent isotropic thermal parameter of their carrier atoms. Weights were optimised in the final refinement cycles. CCDC-178112 (**3**), -178111 (**4**), -178113 (**5**) contain the supplementary crystallographic data for this paper. These data can be obtained free of charge at www.ccdc.cam.ac.uk/conts/retrieving.html or from the Cambridge Crystallographic Data Centre, 12, Union Road, Cambridge CB2 1EZ, UK; [Fax: (internat.) + 44-1223/336-033; E-mail: deposit@ccdc.cam.ac.uk].

HRS Measurements of the First Hyperpolarisabilities: The measurements at a wavelength of 1500 nm were carried out as described in ref.[23] Instead of the third harmonic (355 nm) generated from an Nd:YAG laser with a wavelength of 1064 nm the optical parametric oscillator (OPO)[33] in use was pumped with the second harmonic (532 nm). The signal intensity at 824 nm and the fundamental at 532 nm were removed from the Idler using dichroic mirrors (HR 650−850 and HR 532), a green light and a silicon filter (transparent > 1000 nm). An additional Glan-Taylor polarizer ensured the vertical polarisation of the beam into the measurement cell. Measurements were performed with ca. 10^{-4} to 10^{-6} M solutions of **5**, **7** and **8** in CH_2Cl_2. The validity of Beer's law was proven by UV/Vis measurements of samples with corresponding concentration. Disperse Red 1 (DR1) was used as an external standard with a value of β_{1500}(DR1) = 70 × 10^{-30} esu. This value was obtained by comparing the slopes of the reference in CH_2Cl_2 and $CHCl_3$ to obtain the ratio of β_{solute}.[27] Using the value $\beta(CHCl_3)$ = 80 × 10^{-30} esu[24] the hyperpolarisibility of DR1 in CH_2Cl_2 is estimated to be 70 × 10^{-30} esu. The effect of the refractive indices of the solvents was corrected using the simple Lorentz local field.[28]

Acknowledgments

This work was supported by the European Union through TMR Network Contract No. ERBFMRX-CT98-0166 and COST D14/0008/99, the Deutsche Forschungsgemeinschaft HE 1309/3-4 and the Fonds der Chemischen Industrie.

---

[1] [1a] D. J. Williams, *Angew. Chem.* **1984**, *96*, 637−651; *Angew. Chem. Int. Ed. Engl.* **1984**, *23*, 690−703. [1b] R. W. Boyd in:

Nonlinear Optics, Academic Press, Inc., **1992**; G. H. Wagnière in: *Linear and Nonlinear Optical Properties of Molecules*, VCH, Weinheim, **1993**. [1c] P. N. Prasad, D. J. Williams in: *Nonlinear Optical Effects In Molecules & Polymers*, Wiley & Sons, New York, **1991**. [1d] H. S. Nalwa, S. Miyata (Eds.) in: *Nonlinear Optics of Organic Molecules and Polymers*, CRC Press, New York, **1997**. [1e]J. C. Calabrese, L.-T. Cheng, J. C. Green, S. R. Marder, W. Tam, *J. Am. Chem. Soc.* **1991**, *113*, 7227−7232. [1f] D. R. Canis, M. A. Ratner, T. J. Marks, *J. Am. Chem. Soc.* **1990**, *112*, 8203−8204. [1g] D. R. Canis, M. A. Ratner, T. J. Marks, *J. Am. Chem. Soc.* **1992**, *114*, 10338−10357. [1h] D. R. Canis, M. A. Ratner, T. J. Marks, *J. Am. Chem. Soc.* **1994**, *116*, 195−242. [1i] S. Barlow, H. E. Bunting, C. Ringham, J. C. Green, G. U. Bublitz, S. G. Boxer, I. W. Perry, S. R. Marder, *J. Am. Chem. Soc.* **1999**, *121*, 3715−3723. [1j] T. J. Marks, M. A. Ratner, *Angew. Chem.* **1995**, *107*, 167; *Angew. Chem. Int. Ed. Engl.* **1995**, *34*, 155−174. [1k] N. J. Long, *Angew. Chem.* **1995**, *107*, 37−56; *Angew. Chem. Int. Ed. Engl.* **1995**, *34*, 21−38. [1l] H. S. Nalwa, *Appl. Organomet. Chem.* **1991**, *5*, 349−377. [1m] I. R. Whittall, A. M. McDonagh, M. G. Humphrey, M. Samoc, *Adv. Organomet. Chem.* **1998**, *42*, 291−362. [1n] T. Verbiest, S. Houbrechts, M. Kauranen, K. Clays, A. Persoons, *J. Mater. Chem.* **1997**, *7*, 2175−2189. [1o] B. J. Coe, S. Houbrechts, I. Asselberghs, A. Persoons, *Angew. Chem.* **1999**, *111*, 377−380; *Angew. Chem. Int. Engl. Ed.* **1999**, *38*, 366−369. [1p] T. Kondo, S. Horiuchi, I. Yagi, S. Ye, K. Uosaki, *J. Am. Chem. Soc.* **1999**, *121*, 391−398.

[2] [2a] T. Farrell, T. Meyer-Friedrichsen, J. Heck, A. R. Manning, *Organometallics* **2000**, *19*, 3410−3419. [2b] T. Farrell, A. R. Manning, T. C. Murphy, T. Meyer-Friedrichsen, J. Heck, I. Asselberghs, A. Persoons, *Eur. J. Inorg. Chem.* **2001**, 2365−2375.

[3] T. Farrell, T. Meyer-Freidrichsen, M. Malessa, C. Wittenburg, J. Heck, A. R. Manning, *J. Organomet. Chem.* **2001**, *625*, 32−39.

[4] M. B. Hall, R. F. Fenske, *Inorg. Chem.* **1972**, *11*, 768−775.

[5] C. P. Casey, M. S. Konings, S. R. Marder, Y. Takezawa, *J. Organomet. Chem.* **1988**, *358*, 347−361.

[6] S. M. LeCours, H.-W. Guan, S. G. DiMango, C. H. Wang, M. J. Therien, *J. Am. Chem. Soc.* **1986**, *118*, 1497−1503.

[7] T. Farrell, T. Meyer-Friedrichsen, M. Malessa, D. Haase, W. Saak, I. Asselberghs, K. Wostyn, K. Clays, A. Persoons, J. Heck, A. R. Manning, *J. Chem. Soc., Dalton Trans.* **2001**, 29−36.

[8] [8a] A. E. Asato, R. S. H. Liu, V. P. Rao, Y. M. Cai, *Tetrahedron Lett.* **1996**, *37*, 419−422. [8b] J. N. Woodford, C. H. Wang, A. E. Asato, R. S. H. Liu, *J. Chem. Phys.* **1999**, *111*, 4621−4628.

[9] G. Iftime, P. G. Lacroix, *Tetrahedron Lett.* **1998**, *39*, 6853−6856; P. G. Lacroix, I. Malfaut, G. Iftime, A. C. Razus, K. Nakatoni, J. A. Delaire, *Chem. Eur. J.* **2000**, *6*, 2599−2608.

[10] [10a] R. Herrmann, B. Pedersen, G. Wagner, J-H. Youn, *J. Organomet. Chem.* **1998**, *571*, 261−266. [10b] R. Herrmann, G. Wagner, C. Zollfrank, in *Electronic Conference on Trends in Chemistry* (Eds.: H. S. Rzepa, C. Leach, J. M. Goodman), CD-ROM, Royal Chem. Soc., Cambridge, **1996**, paper 49.

[11] C. P. Casey, M. S. Konings, S. R. Marder, *J. Organomet. Chem.* **1988**, *345*, 125−134.

[12] H. Wong, T. Meyer-Friedrichsen, T. Farrell, C. Mecker, J. Heck, *Eur. J. Inorg. Chem.* **2000**, 631−646.

[13] M. Nitay, W. Priester, M. Rosenblum, *J. Am. Chem. Soc.* **1978**, *100*, 3620−3622.

[14] K. Hafner, C. Bernhard, *Liebigs Ann. Chem.* **1959**, *625*, 108−123.

[15] E. C. Kirby, D. H. Reid, *J. Chem. Soc.* **1960**, 494−501.

[16] [16a] S. R. Marder, D. N. Beratan, L.-T. Cheng, *Science* **1991**, *252*, 103−106. [16b] S. R. Marder, G. B. Gorman, F. Meyers, J. W. Perry, B. Bourhill, J.-L. Brédas, B. M. Pierce, *Science* **1994**, *265*, 632−635. [16c] F. Meyers, S. R. Marder, B. M. Pierce, J.-L. Brédas, *J. Am. Chem. Soc.* **1994**, *116*, 10703−10714. [16d] S. R. Marder, B. Kippelen, A. K.-Y. Jen, N. Peyghambarian, *Nature* **1997**, *388*, 845−851. [16e] J.-L. Brédas, *Adv. Mater.* **1995**, *7*, 263−274.

[17] [17a] G. M. Dawkins, M. Green, J. C. Jeffrey, C. Sambale, F. G. A. Stone, *J. Chem. Soc., Dalton Trans.* **1983**, 499−509. [17b] M. Watanabe, I. Motoyama, T. Takayama, *J. Organomet. Chem.* **1996**, *524*, 9−18. [17c] S. Barlow, L. M. Helling, M. W. Day, S. R. Marder, *Chem. Commun.* **1999**, 1567−1568. [17d] A. I. Yanovsky, Y. T. Struchkov, A. Z. Kreindlin, M. I. Rybinskaya, *J. Organomet. Chem.* **1989**, *369*, 125−130.

[18] [18a] C. P. Casey, M. Konings, R. E. Palerm, R. E. Colborn, *J. Am. Chem. Soc.* **1985**, *107*, 5296−5297. [18b] C. P. Casey, M. S. Konings, S. R. Marder, *Polyhedron* **1988**, *7*, 881−902; M. Etienne, J. Talarmin, L. Toupet, *Organometallics* **1992**, *11*, 2058−2068.

[19] S. Barlow, S. R. Marder, *Chem. Commun.* **2000**, 1555−1562.

[20] [20a] J. L. Oudar, s. S. Chemla, *Chem. Phys.* **1977**, *66*, 2664−2668. [20b] E. Hendrickx, K. Clays, C. Dehu, J. L. Brédas, *J. Am. Chem. Soc.* **1995**, *117*, 3547−3555.

[21] K. Clays, A. Persoons, *Rev. Sci. Instrum.* **1992**, *63*, 3285−3289.

[22] J. J. Wolff, R. Wortmann, *Adv. Phys. Org. Chem.* **1999**, *32*, 121−138.

[23] S. Stadler, R. Dietrich, G. Bourhill, C. Bräuchle, A. Pawlik, W. Grahn, *Chem. Phys. Lett.* **1995**, *247*, 271−276.

[24] C. Lambert, G. Nöll, E. Schmälzlin, K. Meerholz, C. Bräuchle, *Chem. Eur. J.* **1998**, *4*, 2129−2135.

[25] K. Clays, E. Hendrickx, T. Verbiest, A. Persoons, *Adv. Mater.* **1998**, *10*, 643−655.

[26] [26a] J. J. Wolff, R. Wortmann, *J. Prakt. Chem.* **1998**, *340*, 99−111. [26b] S. Stadler, R. Dietrich, G. Bourhill, C. Bräuchle, *J. Phys. Chem.* **1996**, *100*, 6927−6934.

[27] T. Kodaira, A. Watanabe, O. Ito, M. Matsuda, K. Clays, A. Persoons, *J. Chem. Soc., Faraday Trans.* **1997**, *93*, 3039−3044.

[28] C. Lambert, W. Gaschler, E. Schmälzlin, K. Meerholz, C. Bräuchle, *J. Chem. Soc., Perkin Trans. 2* **1999**, 577−587.

[29] G. J. Kubas, *Inorg. Chem.* **1983**, *22*, 692−694.

[30] G. M. Sheldrick, *SHELXS-86 Program for crystal structure determination*, University of Göttingen, Germany, **1986**.

[31] G. M. Sheldrick, *SHELXL-93 Program for crystal structure refinement*, University of Göttingen, Germany, **1993**.

[32] G. M. Sheldrick, *SHELXL-97 Program for crystal structure refinement*, University of Göttingen, Germany, **1997**.

[33] Paralite Optical Parametrical Oscillator, LAS GmbH.

Received January 23, 2002
[I02041]